Mixed Membrane Langmuir-Blodgett Molecular Assemblies: A Solid-State Colorimetric Film Sensor for Lead(II) and Mercury(II)

[1]M. Akhila Maheswari, [2]D. Prabhakaran, [3]C. Subhashini

[1]Department of Chemistry (S&H), VelTech MultiTech Dr RR Dr SR Engg. College, Chennai 600062, Tamil Nadu, India,
[2]School of Advanced Sciences, Chemistry Division, Vellore Institute of Technology (VIT) – University Chennai Campus, Chennai 600127 Tamil Nadu, India.
Email: [1]akhila.maheswari@gmail.com, [2]prabhakaran.d@vit.ac.in

[Received 11th Nov. 2014, Accepted 22nd Nov. 2014]

Abstract — Organized Langmuir-Blodgett molecular assemblies of 4-dodecyl-6-(2-thiazolylazo)resorcinol are transferred onto microscopic glass slides to serve as an efficient ion-sensing probe. The chromo-ionophore film sensor exhibits a visible color transition series, from an initial yellowish orange to a final deep purple and a bright bluish violet, respectively, for submicromolar levels of Pb^{2+} and Hg^{2+}. Intact positioning of probe layers, under conditions of deterioration, has been sustained using a polymer monolayer. Isotherm (surface pressure (π)-area (A)) plots show precise control of sensor/polymer film thickness and homogeneity. Sensor characterization and its ion interaction surface morphology are examined using attenuated total reflectance (ATR)-FT-IR specbetroscopy, X-ray photoelectron spectroscopy (XPS), atomic force microscopy (AFM), and scanning electron microscopy (SEM). Quantitative analyte sensing and changes in the probe's intrinsic optical properties are followed by absorption spectroscopy. The sensor presents a reliable detection and quantification limits of 0.026 and 0.048 µM for Pb^{2+}, and 0.039 and 0.076 µM, for Hg^{2+}. High selectivity and rapid response are achieved with the probe membrane; its ion-sensing behavior has been investigated thoroughly using simulated and real samples. To the best of our knowledge, this is the first reported demonstration of a colorimetric Pb^{2+} and Hg^{2+} sensor using Langmuir-Blodgett technology.

Keywords: Langmuir-Blodgett, ion sensing probe, Lead(II), mercury(II)

I. INTRODUCTION

Heavy metal ions are environmental toxins which disturb the normal functioning of vital organs and thereby impart adverse biological effects. Incidents involving lead (II) and mercury (II) ions effects on humans are reported frequently. Alarming amounts of these toxic anthropogenic ions are emitted into soils and aquatic environments; they are categorized as non-biodegradable pollutants. For instance, discharged mercury(II) from effluents undergoes a series of biogeochemical transformations to toxic organo-mercury species, like CH_3Hg^+ and $(CH_3)_2Hg$, which are transmitted easily through the food chain [1]-[2]. The compounds accumulate in carnivores and persist in the environment. Seafood containing mercury, when eaten by pregnant women, promotes fetal developmental disorders, especially those of the brain and nervous system, because of selective inhibition of protein and amino acid absorption into brain tissue [3]. Being a potential neurotoxin and nephrotoxin, mercury ions in blood serum can affect normal heart function, alter the vascular response to norepinepherine and potassium chloride, and block the entry of calcium ions into the cytoplasm [4]. In addition, human exposure to lead-contaminated sources beyond permissible limits can cause chronic inflammation of the kidney and heart, aside from inducing nervous and gastrointestinal disorders, and impairment of the immune and reproductive systems [5]-[6]. For those reasons, efforts in identifying Pb^{2+} and Hg^{2+} ions in contaminated industrial effluents, water supplies, and environmental sources are important for limiting human exposure and furthering environmental protection.

Over the last few years, advanced sensing equipment has become increasingly demanded for monitoring these metal ions in various matrices. Industrial and technological advancements have provided many commercially available instruments, but these analytical tools require an elaborate laboratory setup, such as a signal transducer for species recognition, or a sample clean-up procedure for reliable analyses. Sensor technology is a rapidly growing area of research that is expected to improve methods of on-site field analysis [7]-[8]. Development of reversible, fast, portable, extremely durable, inexpensive, and reusable analytical probes has persisted as an important goal of the scientific community. Optical ion-sensors based on

chromoionophores, [9]-[15] fluorophores, [16]-[24] electrochemistry, [25]-[28] and enzyme inhibitions [29]-[30] for various toxic cationic and anionic species have been reviewed, but they are normally associated with certain limitations: a tedious synthesis route, complicated analysis, delayed signal response, insufficient selectivity, and low sensitivity. The magnitude of the problems associated with environmental monitoring and waste management has signaled a need for the use of analytical methods that are more rapid and cost effective. Fabrication of solid-state colorimetric sensors for visual detection is much less advanced, even though these sensors can allow on-site real-time qualitative and semi-quantitative detection without sophisticated analytical instruments. Despite the advantages, there appears to be only limited usage of strip tests for environmental monitoring and waste management due to factors such as, low sensitivity, slow diffusion limitations and high cost factor. However, developments and technical refinements in this field is being investigated using different techniques such as, sol-gel membranes, mesoporous monoliths, molecular imprinted polymers, nano-thin film techniques, etc. [31-35]. Among those, the present study specifically examines the use of nano assemblies of organic molecular structures, under the explored area of sensor fabrication, especially visual sensing.

Langmuir-Blodgett (L-B) thin film techniques have been acknowledged as important tools for nanotechnology, offering several advantages over standard sensor fabrication techniques [36-38]. The technology enables molecular engineering that facilitates specific orientation and ordered molecular structures for rapid signal response. The L-B molecular assemblies have attracted considerable interest in the areas of microelectronics, friction control, photovoltaic devices, and sensors [35]. Although L-B monolayers' properties are well established in the field of electronics, a handful of chemical and bio-sensors have been developed related to pH and gas sensors, molecular recognition, etc. Nonetheless, few reports have described their application as visual ion-sensors, especially in the areas of toxicity measurements. We have therefore conceptualized the development of a smart optical sensor that highlights the potential of a chromo-ionophore molecular assembly as a micro-analytical tool for monitoring target toxic ions that are present at parts-per-billion (μg dm^{-3}, ppb) concentrations. To achieve this, 4-n-dodecyl-6-(2-thiazolylazo) resorcinol was chemically synthesized and transferred as monolayers to serve as a visual sensing probe for trace Pb^{2+} and Hg^{2+}ions. The sensor color series was selective for Pb^{2+} and Hg^{2+} ions, without inordinate interference from other heavy metal ions. In addition, excellent sensor reversibility was observed during immersion of the metal complexed sensor strip in dilute HCl solution; the action resembled that of a binary on/off sensor. This article describes the effectiveness of Langmuir-Blodgett film assembly in the unexplored area of colorimetric ion-sensing and highlights its principles and technology, while suggesting future uses. The derived sensor is anticipated for use in determination of lead and mercury contaminants in water supplies, effluent streams, and in specific processes.

II. EXPERIMENTAL

a. Materials

Two chemicals used for probe synthesis were purchased: 4-dodecylresorcinol (Aldrich Chemical Co. Inc. Milwaukee, USA) and 2-aminothiazole (Tokyo Kasei Kogyo Co. Tokyo, Japan). Other chemicals and reagents were of analytical grade pure and were used without further purification (Wako Pure Chemical Industries Ltd., Osaka, Japan). The amphiphilic polymer, polyvinyl-N-octadecyl carbamate (mol. wt. ca. 40000), which was used for probe protection, was obtained from Aldrich Chemical Co. Inc. (Milwaukee, USA). For monolayer fabrication, the water subphase was purified using a water purifier (SA-2100E1; Eyela Tokyo, Japan) water deionizer purification unit, with a nominal resistivity of 18.2 MΩ cm. Individual metal ion solutions were prepared from their corresponding AAS grade (1000 mg dm^{-3}) stock solutions purchased from Wako Pure Chemical Industries Ltd. (Osaka, Japan). Good's buffers (0.2M each of, 3-morpholinopropane sulfonic acid (MOPS)-NaOH, 2-(cyclohexylamino) ethane sulfonic acid (CHES)-NaOH, and N-cyclohexyl-3-aminopropane sulfonic acid (CAPS)-NaOH) were obtained from Dojindo Laboratories (Kumamoto, Japan). Precleaned micro-slide S-111 type (Matsunami Glass Ind. Ltd., Japan) glass plates of specific dimensions (38×13 mm) and thickness (0.8–0.1 mm) were used for solid-state sensor fabrication.

A. Instrumentation

The structure of probe molecule was characterized using ^{1}H and ^{13}C NMR (Varian 400-MR; Varian Inc., Japan) and an FT-IR spectrometer (IRPrestige-21; Shimadzu Corp., Japan). The purity of the synthesized probe molecules was tested chemically using an elemental analyzer (JM10 Microcorder; J-Science Group, Japan). L-B monolayers were generated using a constant moving wall method (NL-LB200-MWC; Nippon Laser and Electronics Lab., Japan) L-B trough (size 80 × 585 mm, capacity 800 cm^{3}) film deposition system. A portable pH/Ion meter (D-53; Horiba Kyoto, Japan) was used for measuring water (subphase) pH, which was normally maintained between pH 6.5–7.0, for all experiments. Changes in the sensor optical properties were monitored using a UV-3150 (Shimadzu Corp., Japan) model double-beam UV-Vis absorption spectrophotometer equipped with a detachable solid sample holder compartment.

Metal ion sensing was performed through batch equilibration using a mechanical shaker (BT-100;

Yamato Co. Ltd., Japan) with a built-in water bath incubator. The residual aqueous phase metal ion concentrations after phase equilibration were determined with an inductively coupled plasma atomic emission spectrometer (ICP-AES, SPS-1500; Seiko Instruments Inc., Japan). Buffer solutions were adjusted to ambient pH values using a micro-computerized pH/Ion meter (F-24; Horiba, Kyoto, Japan).

B. Synthesis and characterization of ion-sensing probe

The amphiphilic chromophore was synthesized chemically via standard diazonium chemistry. Into a 100 cm^3 solution of 0.4M H_2SO_4, 2-aminothiazole (15 g, 0.15 mol) was dissolved uniformly and stirred for 1 h at 2°C. To that homogeneous mixture, an ice-chilled 100 cm^3 solution of sodium nitrite (10.8 g, 0.16 mol) was added drop-by-drop and stirred vigorously for 2 h, under freezing conditions. The excess nitrous acid was tested using starch-iodide paper and quenched with urea. An equimolar ratio of 4-dodecylrescorcinol (41.8 g, 0.15 mol), dissolved in 50 cm^3 volume of C_2H_5OH-(0.5%) NaOH (3:1) mixture, was added to the diazotate at 1–3°C. The coupling reaction was facilitated by maintaining the solution pH around 6.5. After completing addition, the mixture was refrigerated overnight and the desired product was observed as a dark reddish precipitate in the mother liquor. The solid product was filtered and purified by successive washing with hot and cold water before recrystallization from 70% ethanol. (Found: C, 64.69; H, 8.05; N, 10.71; S, 8.19. $C_{21}H_{31}O_2N_3S$ requires C, 64.78; H, 7.97; N, 10.79; S, 8.22%). ^{1}H NMR (400 MHz, $CDCl_3$): δ 0.88 (3H, t, J 7.0), 1.26–1.37 (16H, m, 8×CH_2), 1.63 (2H, p, J 7.3), 2.58 (2H, t, J 7.6), 6.41 (1H, s, Ph), 7.21 (1H, s, Ph), 7.32 (1H, d, J 3.4, Tz), 7.88 (1H, d, J 3.4, Tz), 5.02 (2H, s(b), OH). (Ph and Tz denote phenyl and thiazole groups). ^{13}C NMR (100 MHz, $CDCl_3$): δ 14.1 (CH_3), 22.7 (CH_2), 29.0 (CH_2), 29.4 (CH_2), 29.5 (CH_2), 29.6 (CH_2), 29.6 (CH_2), 29.7 (CH_2), 29.7 (CH_2), 29.7 (CH_2), 29.7 (CH_2), 31.9 (CH_2), 76.2 (Ph, C), 113.1 (Ph, CH), 132.3 (Ph, C), 138.1 (Ph, CH), 119.6 (Tz, CH), 143.2 (Tz, CH), 158.6 (Tz, C), 167.1 (Ph, C-OH), 178.4 (Ph, C-OH). UV-Vis: λ_{max}(75% EtOH)/nm 485 (ε / dm^3 mol^{-1} cm^{-1} 24700). The molecular structure of the probe, 4-dodecyl-6-(2-thiazolylazo)resorcinol (DTAR), and the polymer, polyvinyl-N-octadecylcarbamate (PVOC), are shown in Fig. 1.

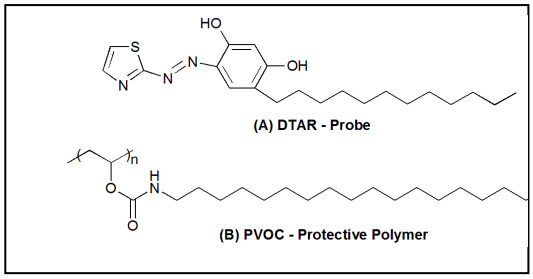

Fig. 1. structure of, (A) amphiphilic probe and (B) surface-protecting polymer.

C. Sensor fabrication and ion-sensing methodology

For isotherm measurements and L-B film preparation, the coating materials, 1 mM of 4-dodecyl-6-(2-thiazoylazo) resorcinol and polyvinyl-N-octadecylcarbamate were dissolved respectively in high-purity grade benzene and chloroform. The injected volume for film spreading, depending on the sensor composition, was varied within the optimum range of 85–100 µL. Beyond this volume, molecular segregation of film layers was observed to reduce the energy associated with the high surface-area-to-volume ratio. The spread film was compressed with a constant moving teflon barrier maintained at 10 mm min^{-1} speed to obtain L-B monolayers at the air-water interface. The surface pressure was measured using an electrobalance, which was interfaced to a computer controlled feedback system, with an accuracy of ±0.5 mN m^{-1}. The L-B monolayer films were transferred onto hydrophilic glass substrates, which were pretreated with piranha solution (1:1 H_2SO_4 and 30% H_2O_2 at 70 °C) and the layers were transferred at their target surface pressure. A thermostat was used to control the sub-phase temperature, where the monolayer fabrication was performed at 20°C. Isotherm plots and film deposition, performed either at 25°C or 15°C, engendered no specific changes.

All experiments for ion-sensing were performed at 25–40°C using deionized water. The metal ion concentrations are expressed either as parts-per-million (mg dm^{-3}, ppm), parts-per-billion (µg dm^{-3}, ppb), or in terms of molarity (M). Sensor working conditions were optimized by batch equilibration method: immersion of the sensor strips in buffered analyte solution of 20 cm^3 overall volume.

D. Sensor characterization

The structural features of three-monolayer DTAR molecular assemblies held on a glass substrate were characterized (IRPrestige-21; Shimadzu Corp., Japan) using an ATR (ATR-8000 model)-FT-IR transmission spectrophotometer. Spectral bands were observed at 2913 and 2848 cm^{-1}, which were attributed to CH_2 asymmetric and symmetric stretching modes of the dodecyl alkyl chain. The strong conjugated -C=C-, -C=S, and -N=N- stretching vibrational modes were observed, at 1621, 1493 and 1402 cm^{-1} respectively, that corresponds to the phenyl, thiazole and azo groups. Absorption peaks observed at 3458 and 1653 cm^{-1} were attributed to the -OH stretching and scissoring vibration modes that coincide with Si-OH stretching vibration. Then, XPS analysis of a 7-layer film membrane was performed using a spectrometer (5601ci; Ulvac PHI) equipped with a conventional MgKα X-ray source (14 kV, 400 W). Depth profiles for elements in the surface film were obtained using argon sputtering (2 kV) with an etching rate of ca. 3 nm/min. The sample chamber pressure was maintained under 1 □ 10^7 MPa and the binding energy scales were referenced to the highest

C(1s) line at 285.4 eV. Fig. 2 indicates the inclusion of Pb^{2+} and Hg^{2+} ions in the probe assembly, with active participation from N=N, OH and thiazole sites for ligation

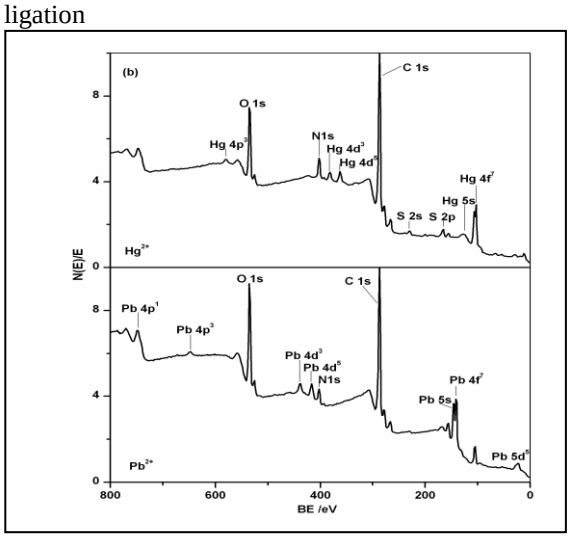

Fig. 2. XPS spectra for a seven-layer DTAR probe obtained after inclusion of Pb^{2+} (bottom) and Hg^{2+} (top) ions, anchored on a SiO_2 substrate.

For assessing the film quality according to the molecular layers transferred on the glass surface, AFM images were obtained (NanoScope IIIa; Digital Instruments, Japan) using AFM tapping mode. An AFM image of the surface etched probe monolayers (withdrawn at π = 28 mN m^{-1}) confirmed the layer by layer assembly pattern, with a smooth peak-valley domain (Fig. 3a). Ion-inclusion imaging at higher resolution revealed the steric influence on the probe structural geometry, forcing a coiling effect on the long dodecyl groups (Fig. 3b). The surface morphology and layer pattern of film membrane after Pb^{2+} and Hg^{2+} interaction were also studied using SEM imaging (Miniscope TM-1000; Hitachi Ltd., Japan) with an acceleration voltage of 15 kV (Fig. 3c).

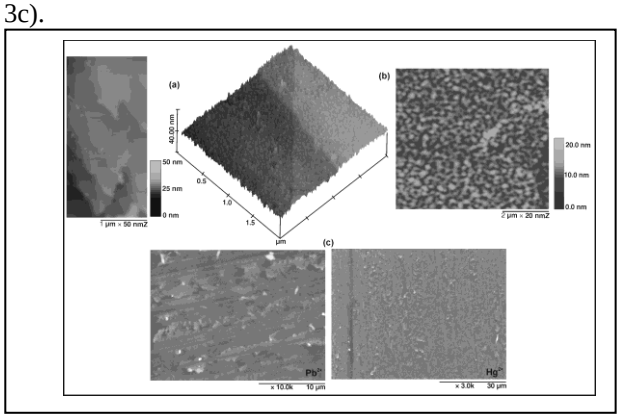

Fig. 3 (a) Layer assembly pattern of a 10-layer L-B film of DTAR and its three-dimensional surface structure morphology by AFM (right); (b) AFM imaging of the metal complexed probe distorted structure, showing the worm-like effect; and (c) SEM image of the surface distributed Pb^{2+} and Hg^{2+} ions, with the probe membrane. The SEM images were taken respectively at different scan areas (10 and 30 μm) with 10000 and 3000 magnifications for Pb^{2+} and Hg^{2+}.

III. RESULTS AND DISCUSSION

E. Isotherm plot and transfer mechanism

The surface pressure-area (π-A) isotherm for the probe (DTAR) and its protecting polymer (PVOC) were measured at the air-water interface to elucidate the monolayer stability and phase transition (Fig. 4a). Isotherms for probe molecules exhibit a single phase transition i.e., from a loosely packed gaseous liquid expanded (G/LE) state to closely packed short-range ordered liquid expanded/liquid condensed (LE/LC) state, with a limiting molecular area of 36.3 $Å^2$, followed by a steep rise until 15.1 $Å^2$, denoting dense packing (with a π value of ca. 37.5 mN m^{-1}), above which the film collapses. These transitions should correspond to the non-planar to planar conformation of the thiazole and phenyl rings, with the dodecyl chain oriented outward from the water surface, with a possible trans orientation of the azo dye, along the sub-phase plane. For a PVOC film, the isotherm shows two phase transitions. At 50.7 $Å^2$, a transition from the gaseous state to the liquid expanded state is observed, which is possibly attributable to the gauche conformation acquired by the octadecyl units. However, with decreasing molecular area, the plot develops a steep rise after 43.3 $Å^2$, which demonstrates the condensed solid (LC) state of molecular close packing and uniform orientation, with a limiting collapse pressure of 45.5 mN m^{-1}. In the context of providing stable probe molecular assemblies, a higher limiting surface pressure was expected from the polymer nanoassemblies, which can ensure greater sensor surface coverage. We studied the influence of surface pressure (π, on the quality of film transfer by measuring the transfer ratio (τ, defined as the area ratio of monolayer occupied on the water surface (A_L) and the solid substrate (A_S), i.e., A_L/A_S, at different surface pressures. The transfer ratio is a key index to determine the film deposition quality, with a recommended value of 1 ± 0.05. For ensuring better film homogeneity and a better film transfer ratio (τ), the probe and polymer monolayers were deposited respectively at a surface pressure of 28 and 40 mN m^{-1}.

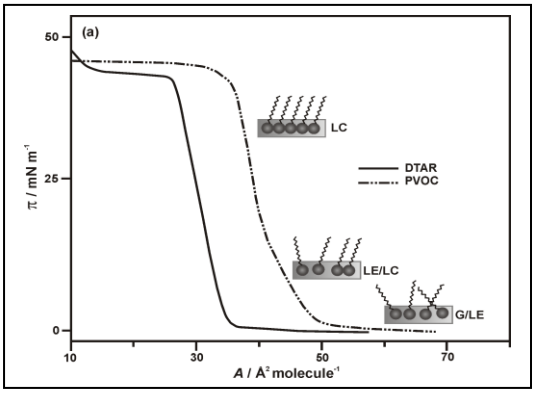

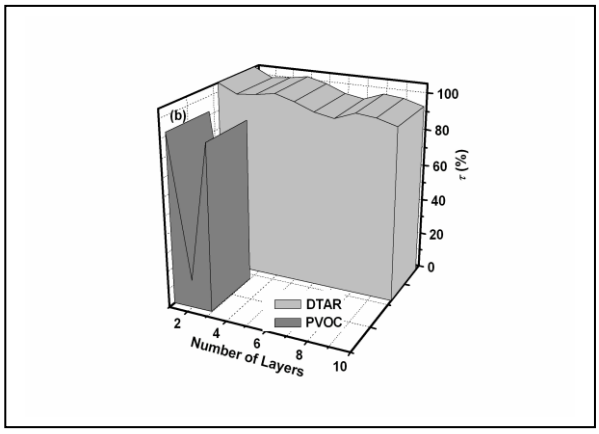

Fig. 4 (a) Isotherm plot for DTAR and PVOC monolayers at pH 6.5 and 20°C on a sub-phase of pure water. Different molecular states are indicated (G, gaseous; LE, liquid-expanded; LC, liquid-condensed). (b) Transfer ratios, τof 10-DTAR on SiO_2 substrate and 3-PVOC monolayers on a probe-mounted SiO_2 substrate.

Fig. 4b shows that the mechanism of probe monolayer transfer involves a homogeneous Y-type deposition pattern (head-to-head and tail-to-tail interaction) on the hydrophilic glass substrate, with a τ of 1 ± 0.05. The polyvinyl-N-octadecylcarbamate monolayer used for sensor shielding exhibits a mixed Y-type film deposition pattern with respective τ values of ≥0.95 and ≤0.15 during up-stroke and down-stroke. The dipper speed for probe transfer was set at 0.15 mm min^{-1} for both up-strokes and down-strokes. For polymer coverage, the dipper was set at 0.1 mm min^{-1} to obtain acceptable and reproducible τ values for specific sensor compositions. Optimizing the sensor fabrication instrumental parameters and the combined use of L-B film polymer composite solves the limitations of using L-B technique with respect to its film quality and stability.

F. Polymer features and sensor workability

A critical feature in designing sensors for use in solution is to ensure that the coating/interface material can be reproducibly and securely attached to the substrate, so that it does not leach into the surrounding medium, nor react with it. The properties of polymer surface coverage on probe monolayers, and their importance were studied by measuring the absorption intensity of a 31-layer probe composite, which was then correlated to a similar probe membrane with an additional polymer film coating. Comparison of the data revealed unaltered signal intensities and a peak profile (λ_{max} ca. 540 nm) in spite of polymer doping, to confirm its spectral non-inference property with respect to the probe's intrinsic optical intensity and also did not interfere in the sensing process. Studies of the influence of solution pH on sensor durability confirmed a moderately stable probe assembly in the regions of near neutrality, irrespective of the adhesive polymer film layer. However, for 6≤ pH ≥8, polymer coverage is apparently necessary because of ligand bleeding from the anchoring substrate. The fragile nature of the outer probe multilayer assembly is the reason predicted for the sensor instability, inspite of a strong head-to-head dipolar interaction of the first layer. During the first probe monolayer transfer, the adhesion interaction of monomolecular films and solid substrate is a heterogeneous process, with a strong molecular interaction for surface adhesion. However, this seems to be a semi-homogeneous phase, with an increasing number of monolayers. The physisorbed outer molecular assemblies are held by a weak interfacial interaction (van der Waals, acid-base, etc.), which is likely to loosen when exposed to extreme working conditions. Introducing a polymer composite on the sensor surface prevents the dislocation of probe molecular assemblies from the solid platform, thereby ensuring stable sensor working conditions even when exposing the film membrane to 0.5 M HCl and NaOH medium. Extensive studies of PVOC film transfer properties and its effect on membrane stability confirmed that a single polymer layer can protect the multilayer probe membrane efficiently. Furthermore, the efficiency of the polymer L-B film in protecting the probe monolayers was tested with surfactants under conditions that can deteriorate the sensor assembly; results showed that a stable sensor system can be useful for practical applications. The surfactants studied individually for stability studies were included alongside matrix tolerance limits during ion-sensing. They are listed in Table 1.

For ion-sensing measurements, a series of sensor assemblies (comprising 10 monolayer DTAR film coated with a PVOC monolayer) were batch-equilibrated individually with 0.5 µM solutions of $Pb^{2+}$and Hg^{2+}; their relative signal response, $\lambda_{605\ nm}$) was monitored at various solution pH. Fig. 5b highlights the sensor working pH range of 7.0–8.5 (using MOPS buffer) for Pb^{2+}, which distinguishes it from Hg^{2+} sensing, which was possible even at pH 5.5 and to sustain to its maximum at pH 6.5. It has been observed that the sensor ion-sensing ability was narrowed between near-neutral to slightly alkaline conditions, which was attributed to the poor acidic properties of the probe molecular assembly. In addition, the tendency of Pb^{2+} and Hg^{2+} ions to undergo partial to complete hydrolysis with increasing alkalinity is a possible reason for the sensor's diminishing ion-sensing behavior after pH ≥ 8.5. Aside from the target ions, visible color patterns and sensing measurements were also extended for 0.25–2.5 µM solutions of other heavy metal ions, which showed marginal response under these conditions. Hence, by manipulating the sensor working conditions, selective and differential sensing of trace Hg^{2+} and Pb^{2+} ions can be achieved on the same sensor kit, thereby shaping the present sensor as an efficient 2-in-1 sensing tool.

G. Sensor film thickness and signal response

The film sensor thickness influenced the visual sensing and phase exchange kinetics of Pb^{2+} and Hg^{2+} ions. A 10-layer molecular assembly of the probe membrane was sensitive to the parts-per-billion level of analytes and showed a visible color pattern. However, an increased number of monolayers impair the sensor sensitivity towards submicromolar-level analytes because of enhanced sensor color contrast. Moreover, this aspect also compromises the signal response because of the poor penetration ability of the metal ions through the dense molecular channels. Using a DTAR10-PVOC1 membrane composite, analytes between 0.05–0.10 ppm can be sensed quantitatively within a time frame of ≤ 600 s, which was reduced to ≥ 420 s for ≥ 0.1 ppm of Pb^{2+} and Hg^{2+} ions at 25°C. A series of experiments were performed to study and measure the spectral changes which occur upon addition of different concentrations of Pb^{2+} and Hg^{2+} ions. The concentration-proportionate signal response for Pb^{2+} and Hg^{2+}, and its visible color pattern on glass anchored DTAR10-PVOC1 membrane are depicted respectively in Figs. 5a and 5b. Spectral profile reveals a smooth decrease in the peak intensity at 540 nm, and the appearance and growth of the peak at 605 nm, upon metal ion complexation. Test strips were read by individuals to make visual comparisons to a reference colour chart (visual readings) and also by using UV-Vis spectrometer. Colorimetric strips reading made by both UV-Vis absorption and visual comparisons were found to be reliable and reproducible.

The influence of the solution temperature on metal ion sensing (0.5 µM) using DTAR10-PVOC1 sensor strips was studied for temperatures of 25–40°C. For a DTAR10-PVOC1 or a system with fewer layers, the rise in solution temperature little influenced the ion-sensing rate because of the high surface area and porosity of the sensor that allows for a high density of binding sites. However, by increasing the monolayers from DTAR10-PVOC1 to DTAR16-PVOC1, the duration for quantitative ion capture was raised to ≥ 600 s at 25°C (Fig. 5c), which, however was reduced drastically to ≥ 400 s at 40°C, for both Pb^{2+} and Hg^{2+} ions. The extended signal response with added monolayers was attributed to the increasing membrane thickness, which renders ion percolation through the molecular assembly difficult. However, with increasing solution temperature, the time-factor was reduced considerably, thereby underscoring the importance of the mechanism of metal ion exchange between the aqueous phase and the sensor material. The rate-limiting step in the metal ion transfer to the receiving phase might be diffusion-controlled across the aqueous diffusive boundary layer, at the membrane-water interface. In this study, raising the internal energy of the aqueous phase through heat transfer enhances the analyte mass transfer through the interface considerably. The time dependent phase exchange kinetics observed for the target analytes with the proposed film strips were studied interms of their diffusion values through the membrane channels. The diffusion coefficient values (25°C, 600 s) and were calculated as 1.51×10^{-12} cm^2 s^{-1} & 0.94×10^{-12} cm^2 s^{-1} for Pb^{2+} and 5.67×10^{-13} cm^2 s^{-1} & 6.82×10^{-12} cm^2 s^{-1} for Hg^{2+}, with D10-PVOC1 & D16-PVOC1 strips, respectively, using eq. (1),

$$D = M\Delta g / C_b t A \quad (1)$$

where D is the diffusion coefficient of metal ions through the membrane of thickness □g at time t, and A is the exposed membrane surface area. In addition, M is the mass of Pb^{2+} and Hg^{2+}, which is defined as $M = C_m V_m$, where C_m is the metal ion concentration in the probe membrane of volume V_m.

The diffusion coefficient values reveal that the kinetics of Pb^{2+} uptake is quite faster when compared to Hg^{2+} ions, which was supported by kinetic measurements. Also, it is inferred that the thickness of film membrane not only played a crucial role in bring out visual colour transition but also on the rate of metal ion transport. In the lower range of sensor detection, a DTAR5-PVOC1 detected 0.005 ppm Pb^{2+} and Hg^{2+} ions, within 450 s at 25°C. However, this low probe content membrane assembly requires a bright background to detect visible color patterns, which, however, is useful for quantitative studies based on the relative changes in the absorption spectra.

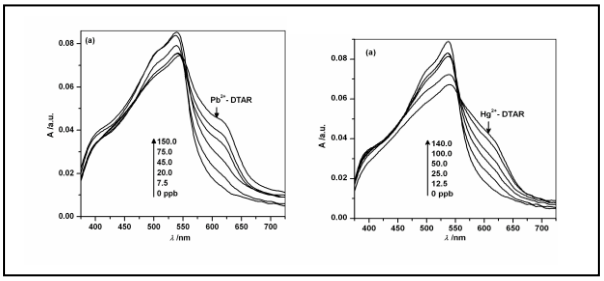

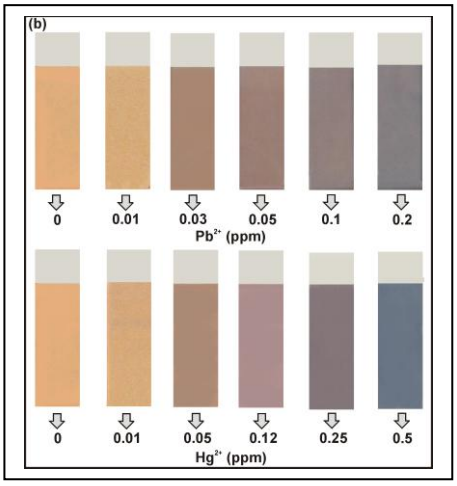

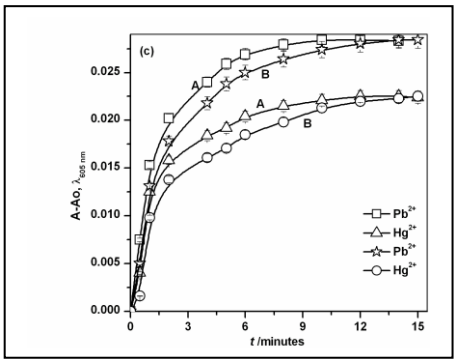

Fig. 5 (a) Absorption spectra of DTAR10-PVOC1 monolayer assembly (λ_{max} ca. 540 nm) for various concentrations of Pb^{2+} and Hg^{2+} ions, with an enhancing spectral band observed at 605 nm. (b) Photographs depicting the concentration proportionate color transition observed on a DTAR10-PVOC1 film sensor for Pb^{2+} and Hg^{2+} ions, against a white background. (c) Signal response observed for both (0.5 µM) Pb^{2+} and Hg^{2+}, with DTAR10-PVOC1 (A) and DTAR16-PVOC1 (B) sensors at 25°C.

H. Sensor performances

An important issue related to sensor feasibility is the selectivity factor, which describes the extent to which a method can determine the analytes without any interference. In real samples, the analytes are normally encapsulated as cationic and anionic species by various matrix compounds. High response speed and confidence in determining analytes in samples of chemically complex matrices are major requirements in such applications. Because the present sensor functions under nearly neutral and slightly alkaline conditions, the influential role played by common electrolyte and complexing species in analyte detection were measured; their levels of tolerances were established and tabulated in Table 1. The scale of sensor ion-selectivity was investigated with possible interfering foreign ions, where alkali and alkaline-earth metal ions were practically non-interfering. With transition metal ions, barring a slight reduction in the sensing kinetics for Pb^{2+} and Hg^{2+} ions, the sensor exhibits good tolerance of major foreign ions including Cu^{2+}, Ni^{2+}, Co^{2+}, and Zn^{2+}, which were found to be competitive for the active site beyond 0.4 ppm at pH ≥ 7.0. Adding a mixture of 0.25 mM citrate and tartrate to the buffer solution eliminates their interference completely, thereby ensuring matrix tolerance up to 100–150-fold excess over Pb^{2+} and Hg^{2+} content. Metal ions of the lanthanide series were totally non-competent for the reactive sites. Other heavy metal ions (depicted in Fig. 6, Table I) did not interfere in the sensing procedure, even at ≤ 5 ppm, which emphasizes the selectivity of the probe monolayers towards the target analytes. The influence of organic matter like humic acid and surfactants (cationic, anionic and non-ionic) that might hamper the sensing process was also investigated. Tolerance towards humic acids (0.0015%) and surfactants (44–85 µM) showed satisfactory findings, as presented in the tolerance table. To further exploit the selectivity aspect, the adopted strategy was to determine trace levels (0.05 ppm) of Pb^{2+} and Hg^{2+} ions from simulated environmental samples containing 100-plus-fold concentrations of matrix ions. Fig. 6a shows the sensor's optical color transition for target ions and its selectivity in different chemical micro-environments. From the interference pattern observed with solid-state film sensor probe it evident that the probe molecular interaction with metal ions in solid phase medium offers some interesting results that are in conspicuous divergence from the solution chemistry of TAR (4-(2-thiazolylazo) resorcinol) dye. Here, we found that the DTAR molecular films mounted on glass solid support offers good selectivity for the target analytes compared to other ions. It was inferred that factors such as, probe molecular orientation on the solid substrate, variation in pKa value of amphiphilic probe, etc., could be the possible reasons for the significant variation in the interference pattern. However, interference from transition ions especially Cu^{2+}, Co^{2+}, Ni^{2+} and Zn^{2+} was observed, which was prominent under high alkaline conditions. But, under the working conditions of Pb^{2+} and Hg^{2+} sensing, only a moderate interference was observed from these foreign ions, which were effectively suppressed.

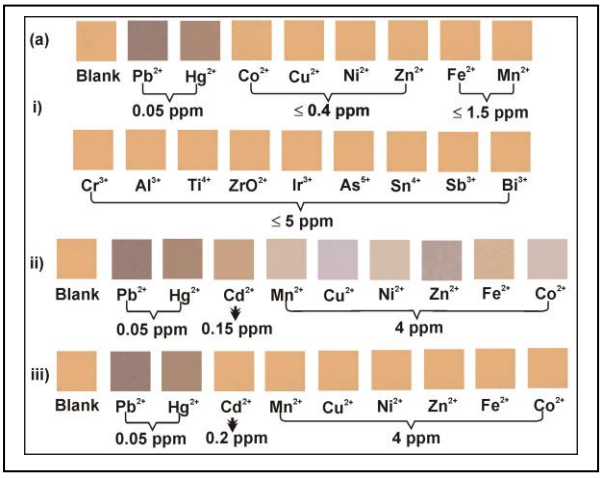

Fig. 6 (i) Selectivity color profile for Pb^{2+} and Hg^{2+} ions on a DTAR10-PVOC1 membrane and its relative comparison with potentially interfering foreign ions, that are present within the sensor tolerance limits, (ii) color transition profile for competing ions, present at 100-fold excess over Pb^{2+} and Hg^{2+} concentrations, and (iii) a similar profile observed after adding 0.4 mM thiosulphate (Cd^{2+}), 0.25 mM of citrate and tartrate to the MOPS buffer solution.

Table. I Tolerance studies

Ions	Tolerance limit for common electrolyte species (mg dm^{-3})					
	NaCl	KNO_3	NaBr	SO_4^{2-}	F^-	PO_4^{3-}
Pb^{2+}	16670	8330	1560	3340	675	450
Hg^{2+}	8100	8500	850	1050	675	490

*Data obtained after using suppressing agents

Ions	Tolerance limit for surfactants (μM)					
	CTAC	TAAC	TEAC	DDAB	SDS	TX-100
Pb^{2+}	64	65	75	68	44	79
Hg^{2+}	52	60	69	70	44	85

Ions	Tolerance limits for interfering metal ions (mg dm^{-3})						
	Cr^{6+}/ Cr^{3+}	Fe^{3+}/ Fe^{2+}	Mn^{2+}	Co^{2+}	Ni^{2+}	Cu^{2+}	Zn^{2+}
Pb^{2+}	12.0/9.6	6.0/4.7*	4.0*	4.3*	4.5*	4.3*	4.0*
Hg^{2+}	10.0/7.0	6.1/5.6*	4.3*	4.7*	4.9*	5.5*	5.1*

Sensitivity studies were performed on DTAR10-PVOC1 film sensors by equilibrating a series of Pb^{2+} and Hg^{2+}concentrations (0.01–1.25 μM); their spectral absorbance at λ_{605} was normalized with respect to the blank sensor. The film sensor gives a linear plot in the respective analyte concentration ranges of 0.023–0.724 μM and 0.037–0.877 μM for Pb^{2+} and Hg^{2+}. The regression equations and correlation coefficients, in the above concentration ranges for Pb^{2+} and Hg^{2+} are, $Y = 0.02C + 0.155$, $r^2 = 0.9996$ and $Y = 0.018C + 0.138$, $r^2 = 0.9994$, respectively, where C is the concentration of the ions. From the normalized calibration plot, the lower limit of detection (L_D) and quantification (L_Q) values were determined using eqs. 2 and 3, which was estimated respectively as 0.026 and 0.048 μM for Pb^{2+} and 0.039 and 0.076 μM for Hg^{2+}. To validate the precision and accuracy of the method, five successive measurements were performed individually for 0.25 μM concentration of Pb^{2+} and Hg^{2+} using D10-PVOC1 strips under optimized experimental conditions. The relative standard deviation for the analysis was calculated as ≤0.211%.

$$L_D = k_1 S_b / m \quad (2)$$

$$L_Q = k_2 S_b / m \quad (3)$$

In those equations, S_b is the standard deviation of the signal response for the blank, m is the slope of the linear calibration range, $k_1 = 3$ and $k_2 = 10$.

Finally, sensor regeneration was tested for its multi-reusability by immersing the metal complexed sensor strips in 20 cm^3 of 0.1 mol dm^{-3} HCl for 300 s. That process resulted in metal ion decomplexation and the sensor was restored to its original color without any loss in its optical intensity (Fig. 7a). The strips were equilibrated in buffered solutions and continued further for ion-sensing. The optical changes in the regenerated sensor strips were almost all of equal intensity to their original performance; that intensity persisted for more than three cycles of repeated usage (Fig. 7b). That sensor reversibility aspect helps to reduce costs of sensor fabrication, thereby facilitating multiple analyses during on-site field measurements, in addition to supporting sensor durability.

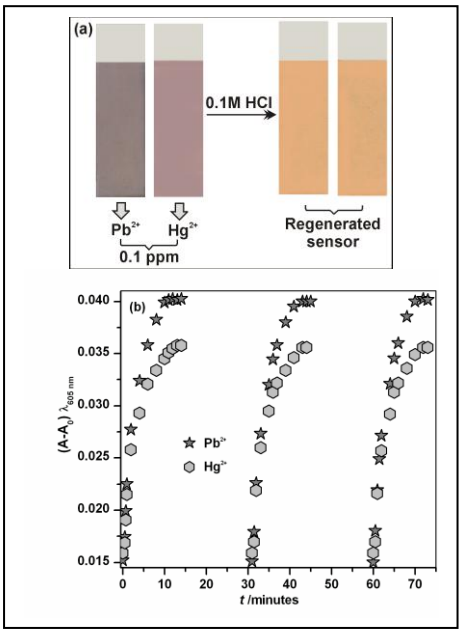

Fig. 7 (a) Regeneration photographic display of Pb^{2+} and Hg^{2+}complexed sensor system, recycled effectively after equilibration with 0.1 M HCl eluant, and (b) recycle response profile for 0.36 μM Pb^{2+} and 0.37 μM Hg^{2+} solutions, on DTAR10-PVOC1 sensor assembly up to three repeated cycles.

I. Ion-sensing from synthetic and real water samples

Quantification of 0.01 mg dm^{-3} levels of Pb^{2+} and 0.015 mg dm^{-3} of Hg^{2+} were tested individually with a stimulated synthetic seawater composite mixture of 3.5% salinity to assess the practical utility of the sensor strip. Spectral analyses of the sensor strip from the calibration plot confirmed the detected amounts to be 10.12 and 14.44 μg dm^{-3} for Pb^{2+} and Hg^{2+}ions, respectively, with a standard deviation value of ≤2.5% for triplicate analysis. In addition, a simulated mixture comprising 2.0 mg dm^{-3} each of Cu^{2+}, Zn^{2+}, Ni^{2+}, Co^{2+}, and Mn^{2+}, and 1.5 ppm each of Ti^{4+}, Zr^{4+}, Bi^{3+}, $Cr^{6+}/^{3+}$, Mo^{6+}, Sn^{2+}, As^{5+}, As^{3+}, Sb^{2+}, and La^{3+} ions was prepared for monitoring sensor selectivity in detecting 0.05 mg dm^{-3} levels of Pb^{2+} and Hg^{2+} ions, with respective estimated values of 49 and 52 μg dm^{-3}. Triplicate measurements were performed on the sensor strips after regeneration, with reproducible values of ≥3.4% deviation.

Finally, four pretreated real sample effluents collected from different sources: food processing factory, semiconductor industry, quartz manufacturing industry, and a local hospital, were used as a precursor sources to test the sensor's practical implementation using real samples. The samples were subjected to ICP-AES analysis and found to contain about 15.7–265 mg dm^{-3} of alkali and alkaline earth metal ions, in addition to traces (0.02–0.083 mg dm^{-3}) of Zn^{2+}, Mn^{2+} and $Fe^{2+/3+}$ ions. Because the real samples had been pretreated, it was decided to adopt an internal standard addition

method to monitor the sensor ion-selectivity to trace-level Pb^{2+} and Hg^{2+}ions that had been spiked to these samples, along with other metal ions listed in Table II. The analytical data indicate the fabricated L-B film sensor as a candidate for monitoring lead and mercury ions from environmental and synthetic samples. There were excellent correlations between the analytical results obtained with the film based test strips and those obtained using the more traditional laboratory methods of ICP-AES and ion-chromatography. This study shows that the use of colorimetric strips for field screening, and in the laboratory, can be a time- and cost-effective alternative to currently used laboratory methods.

TABLE II. ANALYSIS OF Pb^{2+} & Hg^{2+} IN SPIKED REAL SAMPLES

Sample Source	Spiked Amount (mg dm-3)	Amt. Spiked (µg dm-3)		Amt. Found (µg dm-3)	
Food processing factory	1.5 - Co2+, Cu2+, Ni2+, Zn2+, Fe2+; 0.05 - Cr3+/6+, As3+/5+, Mn2+; 0.2 - Sn2+, Sb2+; 10 - Ca2+, Mg2+	0	0	-	-
		10	17.5	09.7 ± 2.3*	17.0 ± 1.7*
		20	25	19.6 ± 2.0*	24.1 ± 3.1*
		50	50	51.2 ± 5.2	48.7 ± 3.4
Quartz manufacturing industrial effluent	0.5 - Si4+; 0.15 - Bi3+, Al3+, Tl+, Ga3+, Ir3+; 0.1 - La3+, Ce4+, Nd3+, Sm3+; 0.05 - W6+, Mo6+, Mn2+; 10 - Ca2+, Mg2+;	15	20	15.6 ± 1.6	20.3 ± 2.0
		25	35	24.8 ± 3.0	35.9 ± 1.9
		50	50	49.3 ± 4.0	49.2 ± 3.5
Semiconductor fabrication facility effluent discharge	0.25 - Bi3+, Al3+, Tl+, Ga3+, Ir3+; 0.1 - La3+, Ce4+, Nd3+, Sm3+; 0.05 - W6+, Mo6+, Mn2+; 10 - Ca2+, Mg2+; 0.5 - Si4+	15	20	14.8 ± 2.1	19.1 ± 3.0
		25	35	25.8 ± 1.5	34.8 ± 4.1
		50	50	50.3 ± 3.8	49.4 ± 5.7
Local hospital effluent	1.75 - Cu2+, Ni2+, Zn2+, Fe2+; 10 - Ca2+, Mg2+	8.5	17.5	8.9 ± 2.1*	19.0 ± 2.9*
		15	15	14.2 ± 3.0*	13.9 ± 2.3*

IV. CONCLUSIONS

To summarize, the article describes an efficient Pb^{2+}/Hg^{2+} sensor that can extend the scope of environmental monitoring using Langmuir-Blodgett methodology. The analytical performance of the L-B sensor was critically assessed, along with its utility, features, and limitations in dealing with different analytical problems. This is believed to be the first attempt at using DTAR nano-assemblies as a sensing probe; it might require further refinements for extension to large-scale production. The time scale of analysis was limited to a few minutes, for which we are now identifying ways by trying with different substrates that could reduce the membrane thickness thus producing selective ion capturing within short contact times. The sensor's durability is an important working parameter that was sustained by choosing the appropriate polymer film with improved adhesion properties to enhance the useful life of the solid-state sensor. The sensor strips are easily portable and storable; they are well-suited to areas of on-site and in-situ field analysis. Based on the United States Environmental Protection Agency's toxicity leaching procedure, the level of Pb^{2+} and Hg^{2+} ions detected and leached from the film sensor were below the agency's regulatory limits. This prototype visual sensor is expected to be useful as a preconcentration tool to produce a liquid desorbent of highly concentrated Pb^{2+} and Hg^{2+} ions. This attempt marks the first step in fabrication of solid-state visual sensors that are compact and well suited to quantitative assessment of toxic metal ion concentrations.

V. ACKNOWLEDGEMENT

The author, D. Prabhakaran gratefully acknowledges Japan Society for the Promotion of Sciences (JSPS) for the fellowship and financial assistance. The authors also acknowledge Dr. Hideyuki Matsunaga and Dr. Hiroshi Nanjo for the support to the above research.

REFERENCES

[1]. H.H. Harris, I. Pickering and G.N. George, "The chemical form of mercury in fish", Science, Vol. 301, pp. 1203, August 2003.

[2]. M. Nendza, T. Herbst, C. Kussatz and A. Gies, "Potential for secondary poisoning and biomagnifications in marine organisms", Chemosphere, Vol. 35, pp. 1875-1885, November 1997.

[3]. E. Coronado, J.R. Galan-Mascaros, C. Marti-Gastaldo, E. Palomares, J.R. Durrant, R. Vilar, M. Gratzel and K.M. Nazeeruddin, "Reversible colorimetric probe for mercury sensing", J. Am. Chem. Soc., Vol. 127, pp. 12351-12356, September 2005.

[4]. E. Oken, R.O. Wright, K.P. Kleinman, D. Bellinger, C.J. Amarasiriwardena, H. Hu, J.W. Rich-Edwards and M.W. Gillman, "Maternal fish consumption, hair mercury, and infant cognition in a U.S. cohort", Environmental Health Perspectives, Vol. 113, pp. 1376-1380, October 2005.

[5]. S.E. Manahan, Environmental Chemistry, Lewis: New York, 6th ed., 1994, pp. 677-679.

[6]. M.J. Derelanko and M.A. Hollinger, CRC Handbook of Toxicology, 2nd ed. CRC: Boca Raton, FL, 1995, pp. 541-550.

[7]. R. Niessner, "Chemical sensor for environmental analysis" Trends Anal. Chem., Vol. 10, pp. 310-316, November 1991.

[8]. K.C. Honeychurch and J.P. Hart, "Screen-printed electrochemical seonsors for monitoring metal

pollutants", Trends Anal. Chem., Vol. 22, pp. 456-469, July 2003.

[9]. M. J. Choi, M.Y. Kim and S.K.Chang, "A new Hg^{2+}-selective chromophore based on calix[4]arenediazacrown ether", Chem. Commun., pp. 1664-1665, September 2001.

[10]. J. Liu and Y. Lu, "A colorimetric lead biosensor using DNAzyme directed assembly of gold nanoparticles" J. Am. Chem. Soc., Vol. 125, pp. 6642-6643, May 2003.

[11]. B. Vaidya, J. Zak, G.J. Bastiaans, M.D. Porter, J.L. Hallman, N.A. Nabulsi, M.D. Utterback, B. Srtzelbicka and R.A. Bartsch, "Chrmomogenic and fluorogenic crown ether compounds for the selective extraction and determination of Hg(II)", Anal. Chem., Vol. 67, pp. 4101-4111, November 1995.

[12]. T. Gunnlaugsson, M. Nieuwenhuyzen, L. Richard and V. Thoss, "The Flurisil catalyzed [1,3]-sigmatropic shift allyl phenyl ethers - An entryway into novel mycophenolic acid analogues", Tetrahedron Lett., Vol. 42, pp. 4725-4728, July 2001.

[13]. J. Liu and Y. Lu, "Stimuli-responsive disassembly of nanoparticles aggregates for light-up colorimetric sensing", J. Am. Chem. Soc., Vol. 127, pp. 12677-12683, August 2005.

[14]. H. Miyaji, W. Sato and J.L. Sessler, "Naked eye detection of anions in dicloromethane: colorimetric anion sensors based on calix[4]pyrrole" Angew. Chem. Int. Ed., Vol. 39, pp. 1777-1780, May 2000.

[15]. M.S. Han and H. Kim, "Naked-eye detection of phosphate ions in water at physiological pH: A remarkably selective and easy-to-assemble colorimetric phosphate-sensing probe", Angew. Chem. Int. Ed., Vol. 41, pp. 3809-2002, 41, 3809.

[16]. W.H. Chang, R.H. Yang and K.M. Wang, "Determination of mercury ion-selecti ve optical sensor based on fluorescence quenching of 5,10,15,20-tetraphenyl porphyrin", Anal. Chim. Acta, Vol. 444, pp. 261-269, October 2001.

[17]. E.M. Nolan and S.J. Lippard, " A turn-on fluorescent sensor for the selective detection of mercuric ion in aqueous media", J. Am. Chem. Soc., Vol. 125, pp. 14270-14271, October 2003.

[18]. M. Plaschke, R. Czolk and J.H. Ache, Fluorimetric determination of mercury with a water-soluble porphyrin and porphyrin-doped sol-gel films", Anal. Chim. Acta, Vol. 304, pp. 107-115, July 1995.

[19]. M.Y. Chae, J. Yoon and A.W. Czarnik, "Chelation-enhanced fluorescence chemosensing of Pb(II), an inherently quenching metal ion", J. Mol. Recognit., Vol. 9, pp. 297-303, July 1996.

[20]. S. Deo and H.A. Godwin, "A Selective, Ratiometric Fluorescent Sensor for Pb^{2+}", J. Am. Chem. Soc., Vol. 122, pp. 174-175, June 2000.

[21]. C.B. Swearingen, D.P. Wernette, D.M. Cropek, Y. Lu, J.V. Sweedler and P.W. Bohn, "Immobilization of a catalytic DNA molecular beacon on Au for Pb(II) detection", Anal. Chem., Vol. 77, pp. 442-448, January 2005.

[22]. T. Gunnlaugsson, M. Glynn, G.M. Tocci, P.E. Kruger and F.M. Pfeffer, "Anion recognition and sensing in organic and aqueous media using luminescent and colorimetric sensors", Coord. Chem. Rev., Vol. 250, pp. 3094-3117, January 2006.

[23]. X. Guo, X. Qian and L. Jia, "A highly selective and sensitive fluorescent chemosensor for Hg^{2+} in neutral buffer aqueous solution", J. Am. Chem. Soc., Vol. 126, pp. 2272-2273, March 2004.

[24]. Q. He, E.W. Miller, A.P. Wong and C.J. Chang, "A Selective Fluorescent Sensor for Detecting Lead in Living Cells", J. Am. Chem. Soc., Vol. 128, pp. 9316-9317, June 2006.

[25]. M.H. Mashhadizadeh and I. Sheikhshoiae, "Mercury(II) ion-selective polymeric membrane sensor based on a recently synthesized Schiff base", Talanta, Vol. 60, pp. 73-80, May 2003.

[26]. W. Yantasee, Y. Lin, T.S. Zemanian and G.E. Fryxell, "Voltammetric detection of lead(II) and mercury(II) using a carbon paste electrode modified with thiol self-assembled monolayer on mesoporous silica (SAMMS)", Analyst, Vol. 128, pp. 467-472, April 2003.

[27]. E. Chow, D.B. Hibbert and J.J. Gooding, Anal. Chim. Acta 2005, 543, 167.

[28]. W. Yantasee, C. Timchalk, K.K. Weitz, D.A. Moore and Y. Lin, "Optimization of a Portable Microanalytical System to Reduce Electrode Fouling from Proteins Associated with Biomonitoring of Lead (Pb) in Saliva", Talanta, Vol. 67, pp. 617-624, June 2004.

[29]. W. Yantasee, Y. Lin, G.E. Fryxell, B.J. Busche, "Simultaneous detection of cadmium(II), copper(II), and lead(II) using a carbon paste

electrode modified with carbamoylphosphonic acid self-assembled monolayer on mesoporous silica (SAMMS)", Anal.Chim. Acta, Vol. 502, pp. 207-212, October 2003.

[30]. J. Liu and Y. Lu, "A general method to convert DNAzymes into fluorescent sensors using catalytic beacon", J. Am. Chem. Soc., Vol. 122, pp. 10466-10467, June 2000.

[31]. L.F. Capitan-Vallvey, C.C. Raya, E.L. Lopez and M.D.F. Ramos, "Irreversible optical test strip for mercury determination based on neutral ionophore", Anal. Chim. Acta, Vol. 524, pp. 365-372, October 2004.

[32]. J.P. Desvergne and A.W. Czarnik, Chemosensors of Ion and Molecule Recognition, NATO ASI Series, Kluwer Academic:Dordrecht, 1997, pp. 205-217.

[33]. S.A. El-Safty, D.Prabhakaran, A.A. Ismail, H. Matsunaga and F. Mizukami, "Nanosensor desogn packages: A smart and compact development for metal ions sensing responses", Adv. Funct. Mater., Vol. 17, pp. 3731-3745, January 2007.

[34]. Oehme and O.S. Wolfbeis, "Optical sensors for the determination of heavy metal ions", Mikrochim. Acta, Vol.126, pp. 177-196, June 1997.

[35]. J. Nagel, U. Oertel, P. Friedel, H. Komber, and D. Mobius, "Langmuir-Blodgett layers from Schiff base copper(II) complexes", Langmuir, Vol. 13, pp. 4693-4698, June 1997.

[36]. M.C. Petty, Langmuir Blodgett Films – An Introduction, Cambridge University Press: New York, 1996.

[37]. K. Ueno, T. Imamura and K.L. Cheng, Handbook of Organic Analytical Reagents, 2nd edn., CRC, Boca Raton, 1992, 205-207.

[38]. D.C. Harris, Quantitative Chemical Analysis, W.H. Freeman: New York, 6th edn., 2003, pp. 601-662.

◈◈◈